

ANTIFUNGAL AND ANTI-AFLATOXIN EFFICACY OF MYCOSYNTHESIS NANOSILVER PARTICLES PRODUCED BY *FUSARIUM* SPECIES: A PHYSICOCULTURAL AND MOLECULAR STUDY

M. I. AI-ZABAN^a, A. R. M. ABD EL-AZIZ^{b,*}, N. SH. ABDELAZIM^a

^aBiology Department, faculty of Science, Princess Nourah bint Abdulrahman University, Riyadh 11474, Saudi Arabia

^bBotany and Microbiology Department, College of Science, King Saud University, Riyadh 1145, Saudi Arabia

Biological method for silver nanoparticles (SNPs) synthesis has been developed to obtain cost effective, clean, nontoxic, and ecofriendly size-controlled nanoparticles. The cell-free culture filtrate (CFF) of 15 isolates belong to three species of *Fusarium* genus, *Fusarium oxysporum*, *Fusarium solani* and *Fusarium verticillioides* were tested to biosynthesis silver nanoparticles (SNPs). This study is important to find out the anti fungal and anti-aflatoxin capabilities of three *Fusarium* spp. The synthesized SNPs were further characterized by UV-Vis spectrophotometry, Fourier transform infrared spectroscopy (FTIR), X-ray diffraction (XRD), transmission electron microscopy (TEM). The physicochemical conditions were screened for maximal SNPs biosynthesis using Plackett-Burman design. All conditions were highly significant ($p < 0.001$). In addition, the SNPs showed notable antifungal activity and potency in thwarting aflatoxin production. Thus, using *Aspergillus flavus* and *A. parasiticus* as a test mycotoxigenic fungi. The utility of fatty acid methyl ester (FAME) profiles could be an additional tool useful for characterization and identification 15 isolates of *Fusarium* spp. Molecular analysis based on the fingerprints obtained through Inter-simple sequence repeat (ISSR) indicated the presence of perfect molecular characterization and high genetic diversity among the *Fusarium* spp. isolates. Cluster analysis using UPGMA method for ISSR markers revealed no clear grouping of the isolates producing and non-producing SNPs. The present study demonstrated that SNPs are a promising approach to control mycotoxigenic fungi; therefore their applications should gained significant importance.

(Received July 27, 2019; Accepted October 26, 2019)

Keywords: *Fusarium* spp., Silver nanoparticles, Antifungal, Anti-aflatoxin, ISSR

1. Introduction

Nanotechnology is emerging as a rapidly growing field with its application in different areas of science and technology. Biological systems for biosynthesis of metallic nanoparticles are safe, low cost, high yield, clean, ecofriendly therefore, the researchers utilized the biological resources as nanofactory [1]. Proposed the term “Myconanotechnology” for the research carried out on nanoparticles synthesis by fungal system. It is the interface between mycology and nanotechnology [2]. Many fungi have the ability to produce silver nanoparticles (SNP) like *Aspergillus terreus* [3], *Penicillium expansum* [4] *Trichoderma Longibrachiatum* [5], *Fusarium oxysporum* [6]. The synthesis of SNPs at nanorange is still a challenge. In order to increase the yield and the shelf-life (stability) of SNPs with minimum investment, it is necessary to optimize the cultural conditions and various physical parameters like pH, light intensity, and temperature [7]. The statistical method for optimization conditions has become a common practice in nanotechnology, for this multivariate design, which allow the simultaneous study of several control variables, is clear choice, good strategy and better than traditional univariate design [8]. Several experimental design strategies, including full-factorial Plackett-Burman; it is often used when more than five independent variables are being investigated [9]. Nanotechnology has led to

* Corresponding author: aabelaziz@ksu.edu.sa

the development of new concepts for agricultural applications especially at plant disease management [10]. As agricultural nanotechnology develops, the potential to provide a new generation of green fungicides and other actives for plant disease management will greatly increasing because of many advantages over conventional chemical fungicides [11]. The green nanofungicide provide us with a new advanced nano-based formulation that remain highly toxicity, long establish, active in the target environment, penetrate the target organism (fungi), cost effective to formulate and manufacture, and preferably possess a new mode of action. previous factors are parameters which define many outstanding properties of nano materials relevant for their use in green nanofungicide application [12, 13]

Aflatoxins (AFs) are toxic secondary metabolites produced by species of *Aspergilli*, especially *Aspergillus flavus* and *A. parasiticus*. AFs produced before and/or during harvest, handling, shipment, and storage [14]. The four majors naturally occurring AFs are known as aflatoxin B1, B2, G1, and G2. AFs have been shown to be potent carcinogens, mutagens, teratogens and hepatotoxic in humans and animals [15]. The recent advancements in agricultural nanotechnology have made SNPs to be novel antifungal, anti-aflatoxin agent and is highly effective against fungal pathogens [16,17]. Sequence analysis of the translation elongation factor 1- α (TEF-1 α) gene, β -tubulin, mitochondrial small subunit (mtSSU), and intergenic spacer (IGS) ribosomal DNA locus have been used to identification *Fusarium* genus [18,19]. The internal transcribed spacer (ITS) sequences have been successfully used to explore inter and intra specific *Fusarium* phylogenetic studies for high resolution data [20,21]. Integrated methods for the identification of fungi are based on the use of phylogenetic and chemotaxonomic markers [22]. Chemotaxonomic markers used in the field of mycology include numerous compounds such as amino acids, fatty acids (FAs) and carbohydrates [23]. FAs are increasingly being used as a chemotaxonomic tool for the identification and classification of fungi [24]. DNA markers allow noncoding DNA sequences to be examined, thereby providing more penetrating insights into population genetic structures. Several molecular technologies are used widely to assess the genetic characterization and genetic diversity of *Fusarium* species, including the analysis of random amplified polymorphic DNA (RAPD), amplified fragment length polymorphisms (AFLP), expressed sequence tags-simple sequence repeats (EST-SSR), sequence-related amplified polymorphisms (SRAP), and inter-simple sequence repeats (ISSR) [25,26]. ISSR is a general term for a genome region between microsatellite loci. It is a fast and inexpensive genotyping technique with a wide range of uses, including the characterization of genetic relatedness among populations of *Fusarium* spp. [27,28].

The present study deals with the extracellular synthesis of SNPs using three *Fusarium* species, *Fusarium oxysporum*, *F. solani* and *F. verticillioides* followed by its characterization and optimization for rapid SNPs synthesis. Furthermore, evaluate their antifungal and anti-aflatoxin against a highly toxigenic strain of *A. flavus* studies have also been carried out, fatty acids were used as chemotaxonomic marker for differentiating between *Fusarium* species. Finally, genetic characterization of these *Fusarium* spp. producing and non-producing SNPs using ISSR markers and evaluate the association between antifungal and anti-aflatoxigenic properties and genotype of isolates.

2. Materials and methods

2.1. Isolation of *Fusarium* spp. from soil samples

Fifteen *Fusarium* spp. isolates were isolated from twenty-four date palm soil samples collected from different localities of Riyadh, in the Kingdom of Saudi Arabia, at a depth of 10–15 cm. Soil samples were collected over the year 2017. Isolation of *Fusarium* spp. was carried out according to [29].

2.2. Identification of fungi

General and specific taxonomic literatures were used for the identification of fungal species: [30,31].

2.3. Genomic DNA extraction

Fusarium spp. isolates were cultured on double layer media in 50 mm Petri dishes, one liquid peptone yeast glucose (PYG, 1200 μ l) and the other solid (potato dextrose agar as a film). DNA extraction was completed according to the protocol [32].

2.4. PCR amplification and sequencing of internal transcribed spacer regions and 5.8S rRNA

Fifteen *fusarium* spp. isolates were molecularly identified on the basis of their internal transcribed spacer regions (ITS1-ITS2) and 5.8S rRNA gene in a similar manner to the study performed by [2]. PCR amplification by primer ITS-1 (5'-TCCGTAGGTGAACCTGCGG3-3') and ITS-4 (5'-TCCTCCGCTTATTGATATGC-3') [33]. PCR amplifications were performed in a Techne TC-312 (Techne, United Kingdom) under conditions specified elsewhere [2]. All experiments were repeated for three times. Amplified products were analysed by electrophoresis on 1% agarose gels in TAE buffer. The amplified product was purified from agarose gel using Wizard® SV Gel and PCR Clean-Up System (Promega, Madison, USA) and sequenced by using an automated ABI-Prism 377 DNA Sequencer (Applied Biosystems Inc., CA, USA). For the confirmation of preliminary identified isolates of *Fusarium* species, nucleotide sequences were compared with those maintained in the GenBank Database through NCBI Blast (<http://www.ncbi.nlm.nih.gov>). Alignment of nucleotide sequences was done using a cluster method W of the MEGA6 software program [34]. A phylogenetic tree was generated based on the percentage difference between the sequences using the neighbor-joining method with the same program.

2.5. Fungal biomass preparation for SNPs biosynthesis

To prepare biomass for biosynthesis studies, the fungus was grown in 250 ml Erlenmeyer flasks aerobically containing 100 ml liquid medium containing (g/l) KH_2PO_4 7.0 g; K_2HPO_4 2.0 g; $\text{MgSO}_4 \cdot 7\text{H}_2\text{O}$ 0.1 g; $(\text{NH}_4)_2\text{SO}_4$ 1.0 g; yeast extract 1.0 g and glucose 15.0 g. Inoculated media were incubated at 28 ± 2 °C and proceeding of a method carried out as described by [35]. Control included the deionized water and AgNO_3 10^{-3} M and the sample replacement deionized water with cell-free filtrate.

2.6. Ultraviolet-Visible Spectrophotometer

UV-Vis is a widespread method of detection of SNP [36]. When bioreduction of SNPs in AgNO_3 solution, this is the main point of reaction and occurred with changing the color of solution. Color change in the reaction mixture (Cell-free filtrate and silver nitrate) was the initial indicator of the formation of SNPs. The solution was monitored by using double beam UV-Vis spectrophotometer, Cintra10e GBC (Victoria, Australia). The absorption spectra of the supernatants were taken between 300 and 700 nm. Scanning was performed after reaction times ranging from 6 hours to 96 hours.

2.7. Transmission electron microscopy (TEM)

TEM was performed on JEOL model JEM-1010, (Tokyo, Japan) within accelerating voltage of 80 kV after drying of a drop of aqueous SNPs on the carbon coated copper. TEM grid samples were dried and kept under vacuum in desiccators before loading on a specimen holder. Determined by TEM as described by [37].

2.8. Fourier transforms infrared

For Fourier transform infrared (FTIR) spectroscopy measurements, the bio-transformed products present in cell-free filtrate after 72 h of incubation were freeze-dried and diluted with potassium bromide in the ratio of 1: 100. FTIR spectrum of samples was recorded on FTIR instrument mode Nicolet 6700 spectrometer of resolution 4 cm^{-1}) attachment. All measurements were carried out in the range of 400– 4000 cm^{-1} at a resolution of 4 cm^{-1} .

2.9 .X-ray diffraction analysis

XRD is an important technique to evaluate the formation of silver nanoparticles and to determine the particle size. The fungal supernatant containing AgNPs was freeze-dried using a

HetoLyophilizer (Heto-Holten, Denmark) and stored in lyophilized powdered form until used for further characterization. The finely powdered sample was analyzed by an X'pert PRO PAN alytical diffract meter using CuK α radiation ($k = 1.54056 \text{ \AA}$) in the range of $20 \leq 2\theta \leq 80 \leq$ at 40 keV.

2.10. Identifying the significant variables using plackett-burman design (PBD)

Screening process was carried out by conducting the experiments to determine which variables significantly affect SNPs production [38,39]. Two level-5 factor experimental blocks were established, A total of 6 independent (assigned) and one unassigned variable (commonly referred to as dummy variable) were screened in Plackett-Burman experimental design of 9 trials. Dummy variable is used to estimate experimental errors in data analysis. Six independent factors were included in the studied pH, salt conc., agitation, incubation time, temperature, the ratio between salt and ECF. For each variable, a high (+1) and low (-1) levels (Table 1). Triple experiments were done for each run with total 27 runs which were applied according to PB design matrix. The response that represents forming SNPs measuring the intensity of absorbance at 420 nm due to the resonance of silver nanoparticles.

Table 1. Experimental range and levels of 6 independent variables in the Plackett-Burman design matrix.

Variables	Level		
	-1	0	1
pH	7	9	11
Temp.	26	28	30
AgNO ₃ concentrate	1	1.5	2
Agitation	100	150	200
Time of incubation	48	72	96
Ratio between ECF volume and AgNO ₃ salt	5:1	10:1	15:1

2.11. Antifungal activity

The fungal growth inhibitory effect of SNPs was tested against two mycotoxigenic fungi, *A. flavus* KSU 107 (peanut) and *A. parasiticus*, C009 (corn) which were kindly obtained from Botany and Microbiology Department, College of Science, King Saud University, Saudi Arabia utilized in the assay. The minimum inhibitory concentration (MIC) test was performed. Spore suspension concentrations were determined using a hemocytometer and adjusted to 2×10^6 spores/mL. One mL of spore suspension was transferred to each well of a petri dish containing potato dextrose agar (PDA) with different concentrations of SNPs. PDA containing the gradual concentrations of (10, 20, 30, 40, and 50 μ g) SNP colloids. The antifungal activity method was performed according to [16].

2.12. Leakage of proteins and DNA

To study the probable mechanism of SNPs affecting cells, the leakage of proteins and DNA from *A. flavus* KSU 107 and *A. parasiticus* C009 cells was studied. Spore suspension solutions of *A. flavus* KSU 107 and *A. parasiticus* C009 (10^6 spore cells/mL) were prepared in saline solution (NaCl, 0.9% w/v). The fungal spore suspensions were incubated for 24 h at 30 °C with synthesized SNPs by *F. oxysporum* PNU43 and *F. solani* PNU54 at their respective MIC values for spore germination inhibition. Control spore suspension sets (without SNPs) were used as blanks. Spore suspension in each case was centrifuged for 15 min at 4000 rpm at 4 °C. The optical density (OD) of the supernatant was read at 280 and 260 nm to estimate the proteins and DNA leaked from the cells.

2.13. Effect of SNPs on fungal production of total aflatoxins

Aflatoxins (B1, B2, G1 and G2) produced by two mycotoxigenic fungi *A. flavus* KSU 107 and *A. parasiticus*, C009. The same quantity (pervious experimental) was add to 250 flasks containing SKMY medium liquid (autoclaved) with (10, 20, 30, 40, and 50 μ g) SNP colloids. then incubated at 27°C for 21 days. After the end of incubation period, B1 was estimated in the liquid culture medium.

2.14. Extraction and measurement of aflatoxins by HPLC

The cultures obtained after incubation were filtered through Whatman number 1 filter paper. The culture filtrates were extracted in the presence of chloroform (1:2 v/v) and procedure apply as [40]. The concentrations of total B1 was quantitatively measured using an HPLC (Perkin Elmer model series 200 UV/VIS) with a C18 column (300 mm x 3.9 mm, 4 μ m). The HPLC system was equipped with a UV detector and fluorescence with 365 nm excitation and 430 emission wavelengths. The mobile phase consisted of methanol: acetic acid: water (20:20:60, v/v/v). The total run time for the separation was approximately 25 min at a flow rate of 1 mL/min [40].

2.15. Extraction of fatty acid methyl ester and analysis:

Fatty acid (FA) extraction and preparation of methyl esters were carried out according to a previously described method [41]. FA methyl esters (FAMES) were analysed by gas liquid chromatography using the Perkin-Elmer Model 910 Gas Chromatograph (Perkin Elmer, Shelton, CT, USA) equipped with a flame ionization detector. Identification (qualitative and quantitative) of FAMES was based on comparison of sample retention times with those of an authentic methyl standard (Sigma Co., St. Louis, MO, USA).

2.16. ISSR-PCR

Genomic DNA extraction was carried out using the method described in an earlier section. Out of the 60 primers used, 28 primers that produced good PCR fragments were employed to specifically amplify *F. oxysporum*, *F. solani* and *F. verticillioides* genomic DNA (Table 2). PCR was carried out as the method described by [42] for *F. oxysporum*, [43] for *F. solani* and [44] for *F. verticillioides*. PCR products were detected with 1.5% agarose ethidium bromide gels in TAE 1x buffer (40 mM Tris-acetate and 1.0 mM EDTA). A 100-bp DNA ladder (Intron Biotechnology, South Korea) was used as the molecular marker.

2.17. Statistical analysis

All data were subjected to statistical analysis. Treatments were compared using Fisher's Least Significant Difference (LSD) analysis. Cluster analysis was performed using SPSS 15 software package. Cluster analysis by the unweighted pair-group method based on the arithmetic mean (UPGMA) was performed using SPSS6.0 software package.

Table 2. ISSR primers used in the present study.

No.	Primer code	Sequence (5'-3')	Ta (°C)	GC content (%)	Ranges of amplified bands (bp)
<i>F. oxysporum</i>					
1	UBC 807	(AG) ₈ T	51	47.1	300-1300
2	UBC 808	(AG) ₈ C	49	52.9	250-1800
3	UBC 809	(AG) ₈ G	52	52.9	250-1500
4	UBC 810	(GA) ₈ T	48	47.1	300-2000
5	UBC 811	(GA) ₈ C	51	52.9	250-2100
6	UBC 818	(CA) ₈ G	49	52.9	250-2200
7	UBC 825	(AC) ₈ T	55	47.1	350-2200
8	UBC 835	(AG) ₈ YC	49	52.8	200-2000
<i>F. solani</i>					
1	UBC 807	(AG) ₈ T	51	47.1	350-1300
2	UBC 808	(AG) ₈ C	49	52.9	250-1800
3	UBC 809	(AG) ₈ G	52	52.9	250-1500
4	UBC 810	(GA) ₈ T	48	47.1	250-2200
5	UBC 811	(GA) ₈ C	51	52.9	250-1900
6	UBC 818	(CA) ₈ G	49	52.9	250-2000
7	UBC 825	(AC) ₈ T	55	47.1	250-2100
8	UBC 835	(AG) ₈ YC	49	52.8	200-2200
<i>F. verticillioides</i>					
1		(AG) ₇ C	41	41	100-1200

No.	Primer code	Sequence (5'-3')	Ta (°C)	GC content (%)	Ranges of amplified bands (bp)
2	UBC 809	(AG) ₈ G	52	52.9	100-1400
3	UBC 810	(GA) ₈ T	48	47.1	100-1800
4	UBC 825	(AC) ₈ T	55	47.1	150-1800
5		(CT) ₈ AC	40	40	200-1800
6		(CT) ₈ GC	43	43	100-1500
7		(ATG) ₆	51	50	200-1800
8		(CCA) ₆	69	68	100-1800

AT = annealing temperature

*ISSR primers sequences published by University of British Columbia

(<http://www.michaelsmith.ubc.ca/services/NAPS/Primerssets/primers-Oct2006.pdf>)

**Y=(C, T)

***Capital letters in ISSR primer sequences denote degenerate sites: B denotes nucleotides C, G, or t; D denotes A, G, or T.

3. Results and discussion

Survey of *Fusarium* spp.

Three species belonging to *Fusarium* genus were obtained from rhizosphere soil samples, *F. oxysporum*, *F. solani* and *F. verticillioides*. *Fusarium* genus is a large, highly diverse complex of morphologically similar anamorphic fungi with multiple phylogenetic origins [45]. This species complex is well represented among fungal communities in different soil types worldwide [46], and is considered a common member of the fungal communities in the date palm rhizosphere [47,48].

Identification of *Fusarium* spp.

The morphological analysis that was initially used to identify isolates revealed that all of the isolates analyzed were including *F. oxysporum* (6 isolates), *F. solani* (5 isolates) and *F. verticillioides* (4 isolates). The isolates were further confirmed by analyzing the ITS1-5.8S-ITS2 regions from these isolates. The amplified *Fusarium* spp. sequences were ranged from 556 to 589 bp. *Fusarium* spp. isolated from rhizosphere soil compared with closely related *Fusarium* spp. in the GenBank (Table 3).

All of *Fusarium* spp. we isolated had 98–99% similarity with the related *Fusarium* spp. listed in the GenBank. Comparison of the ITS1-5.8S-ITS2 regions sequences of these isolates using the BLAST algorithm revealed that all of the isolates belonged to *F. oxysporum*, *F. solani* and *F. verticillioides*.

The sequence of the ITS-rDNA is highly conserved but sufficiently variable among species of *Fusarium* species complex. The ability of the ITS region to differentiate and provide accurate and rapid identification of fusarium genus at the species-level [49]. Specific PCR primers based on ITS sequences for *Fusarium* species complex have been designed based on two single nucleotide polymorphisms (SNPs) present in the ITS region [50].

Table 3. Identification of *Fusarium* species isolated from rhizosphere soil by sequencing of ITS1 and ITS 2 and region of 5.8S rRNA gene compared with sequences listed in the GenBank.

No.	<i>Fusarium</i> species soil fungi			Fungi of gene bank		Identity (%)
	Isolate code	Fungi	Size (bp) of ITS1-5.8S-ITS2 region	GenBank accession number	Fungi	
1	PNU41	<i>F. oxysporum</i>	563	KC215120	<i>F. oxysporum</i>	98%
2	PNU42					
3	PNU43					
4	PNU44					
5	PNU45					
6	PNU46					

No.	<i>Fusarium</i> species soil fungi			Fungi of gene bank		Identity (%)
	Isolate code	Fungi	Size (bp) of ITS1-5.8S-ITS2 region	GenBank accession number	Fungi	
7	PNU51	<i>F. solani</i>	589	MF136402	<i>F. solani</i>	99%
8	PNU52					
9	PNU53					
10	PNU54					
11	PNU55					
12	PNU61	<i>F. verticillioides</i>	556	KX688163	<i>F. verticillioides</i>	98%
13	PNU62					
14	PNU63					
15	PNU64					

Biosynthesis of SNPs using *Fusarium* spp.

The biosynthesis of SNPs using three *Fusarium* spp. was investigated. The reaction of silver nitrate with the filtered cell-free culture, the color of the mixture was gradually changed from pale yellow to dark brown after the addition of silver nitrate and the color change was captured within 96 h (Fig. 1) but *Fusarium* spp.-mediated synthesis of SNPs was observed for first time within 24 h. Color change is the first indication for biological synthesis of SNPs.

Table 4 shows two isolates of *F. oxysporum* were capable of producing SNPs although four isolates failed to produce SNPs. Three of the five *F. solani* isolates were SNPs producers. Two of the four *F. verticillioides* isolates were SNPs producers. In general, seven isolates of *Fusarium* spp. (46%) were able to produce SNPs while eight isolates (54%) failed to produce SNPs.

Soil fungi are often considered as the interesting powerful sources for biological synthesis of metal nanoparticles [51,52]. A many of mechanisms have been proposed, we think two mechanisms or more have overlapping to biological synthesis of SNPs, but all mechanisms depend on protein or/ and enzyme 1) protein involved with NADH-dependent reductase was responsible for the reduction of Ag ions [53]. 2) protein containing amino acid with -SH bonds (cysteine) undergoes dehydrogenation on reaction with silver nitrate to produce silver nanoparticles [54]. 3) hypothetical mechanism depends on a) reduction of silver ions to SNPs by a protein (32 kDa), b), SNPs were capped by a protein that for more stability [55]. 4) aqueous extracts of most fungi containing proteins, alkaloids and many kinds of phenolic which could induce the formation of nanoparticles by serving as reducing agents [6].

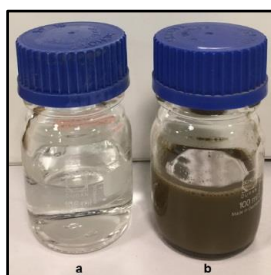


Fig.1. photograph of two bottles containing the aqueous solution of 10^{-3} M AgNO_3 at the beginning of the reaction (a) and after 3 days of reaction (b).

Table 4. Screening of *Fusarium* species isolated from rhizosphere soil for the biogenic synthesis of silver nanoparticles.

No.	Isolate code	Name of isolate	SNPs synthesis
1	PNU41	<i>F. oxysporum</i>	-
2	PNU42		+
3	PNU43		+
4	PNU44		-
5	PNU45		-
6	PNU46		-
7	PNU51	<i>F. solani</i>	+
8	PNU52		+
9	PNU53		-
10	PNU54		+
11	PNU55		-
12	PNU61	<i>F. verticillioides</i>	-
13	PNU62		+
14	PNU63		-
15	PNU64		+

Transmission electron microscopy (TEM)

TEM measurements were used to determine the morphology and shape of nanoparticles (Fig. 2). The TEM image showed variable, but predominantly spherical nanoparticles spherical in shape and are uniformly distributed (monodispersed) without significant agglomeration shape, spherical or nearly spherical and without significant agglomeration.

TEM analysis of morphology and shape of NPs was also carried out to find out the shape and size of SNPs produced by three selected *Fusarium* species, which confirmed the spherical shape of synthesized SNPs. The size of NPs synthesized by all species was in the range of 3-67 nm. The same range of size and shape of SNPs were observed in six *Fusarium* species used for biogenic synthesis of SNPs [2].

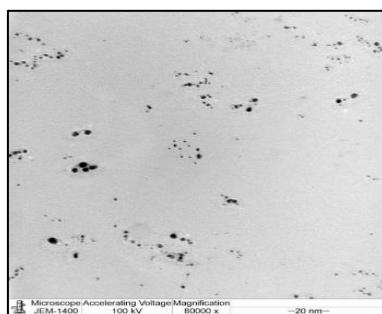


Fig. 2. Transmission Electron Microscopy (TEM) images of synthesized silver nanoparticles by *F. oxysporum* PUN43.

Ultraviolet-Visible Spectrophotometer

UV-Visible spectrum was performed to examine the optical absorbance of SNPs when using *F. oxysporum* PUN43 (Fig. 3). The reaction had run for 6 to 96 hours, showed a strong broad peak at 420 nm called surface plasmon resonances (SPR), which corresponds to indicate the formation of SNPs.

SPR plays a major role in the determination of optical absorption spectra of metal NPs [56]. There is a relation between the plasmon peak and the particle size, as the plasmon peak shifts to longer wavelengths when the particles became larger. When we had lower wavelengths (384–

414) corresponded to 10 to 14 nm particle size [57]. UV spectra at 438 nm wavelength gave particle sizes of 60-80 nm [58].

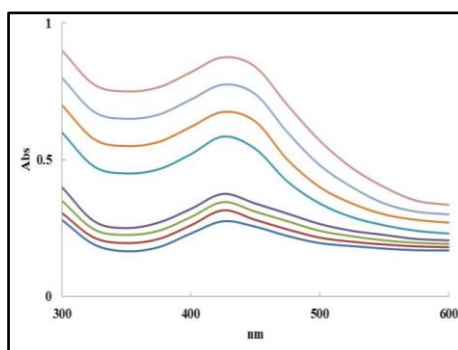


Fig. 3. UV-visible absorption spectrum of AgNPs biosynthesized by *F. oxysporum* PUN43 with different time intervals. — 6 h — 8 h — 10 h — 12 h — 24 h — 48h — 72h — 96 h.

Fourier transforms infrared spectroscopy

FTIR spectroscopy is used to analyze the binding of proteins with silver nanoparticles, and it is possible to characterize the secondary structures involved in the metal nanoparticle-protein interactions. (Fig. 4) shows the FTIR spectrum of a freeze-dried powder of silver nanoparticles formed after 72 h of incubation with the fungus supernatant.

The FTIR spectrum contained two bands at 1636.75 cm^{-1} that correspond to the bending vibrations of the amide I and amide II bands of the proteins [59], and the corresponding stretching vibrations of the primary amines were observed at 3289.48 cm^{-1} . These observations indicate the presence of and the binding of proteins with SNPs, which can lead to the stabilization of the NPs. Thus, the presence of these bands in the FTIR spectra of silver nanoparticles indicate that the secondary structure of the proteins is not affected during the formation of SNPs or by the binding of the proteins with the silver nanoparticles [60].

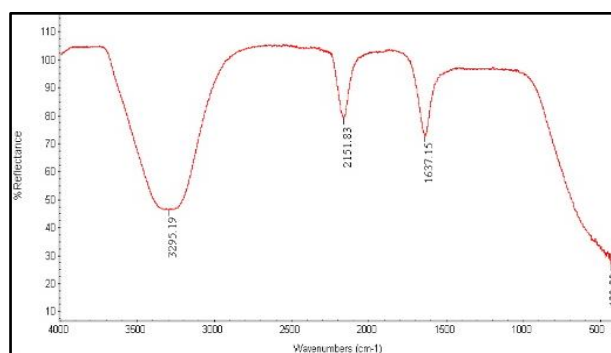


Fig. 4. Fourier Transform Infrared Spectroscopy (FTIR) spectrum of SNPs synthesized by the reduction of Ag^+ ions by *F. oxysporum* PUN43.

X-ray diffraction analysis:

Reflecting the crystalline nature of the SNPs, intense XRD peaks were observed corresponding to the (111), (200), (220) and (311) planes at 2θ angles of 38.43, 46.19°, 58.36°, and 65.11°, respectively (Fig. 5). These results were in good agreement with the unit cell of the face-centered cubic (fcc) structure reported by [55,61].

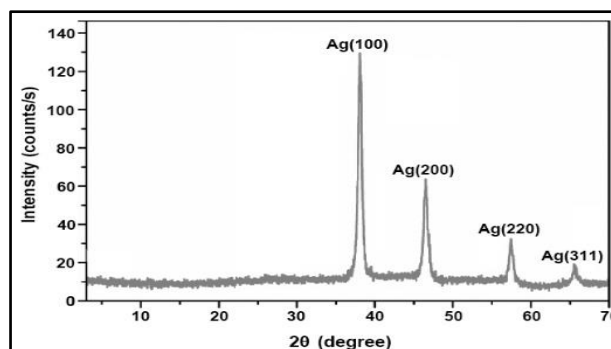


Fig. 5. XRD pattern of as-synthesized SNPs produced by *F. oxysporum* PUN43.

Screening of the significant variables affecting SNPs biosynthesis using plackett-burman design

The results of Plackett-Burman design (PBD) (Table 5) indicate that there was a variation of SNPs biosynthesis in the nine trials in the OD range from 0.57 to 1.88 at 420nm. Based on statistical analysis of nine trials using Plackett-Burman design, trial 6 (pH 7, Temp. 26, AgNO₃ concentrate 2mM, agitation 200, time of incubation 96 h, ratio 5:1) gave the highest production of SNPs.

The analysis of regression coefficients and *t*-value of 6 variables were presented in Table 6. The results showed that pH (confidence level, 99.978%), AgNO₃ concentrate (99.912%), and Ratio (99.953%) were found as the most important significant factors influencing the SNPs biosynthesis. The main effect of each variable (Fig. 6), among the 6 variables pH, AgNO₃ concentrate and ratio showed a highly significant of the effect on SNPs production. Statistical optimization of fermentation conditions using Plackett-Burman design and appear to be a valuable tool for the production of SNPs [38].

Table 5. The Plackett-Burman design matrix representing the values of independent factors and the values of measured response, absorbance at wave length 420nm.

Run	pH	Temp.	AgNO ₃ concentrate	Agitation	Time of incubation	Ratio	DV	Absorbance at 400 nm	Mean ± SD
1	1	1	-1	1	-1	-1	-1	0.98	0.85±62
2	-1	1	1	1	-1	1	-1	0.81	0.61±34
3	-1	1	-1	-1	1	1	1	0.54	0.36±79
4	1	-1	1	-1	-1	1	1	0.68	0.59±12
5	1	1	1	-1	1	-1	-1	1.56	1.48±93
6	-1	-1	1	1	1	-1	1	1.88	1.65±41
7	1	-1	-1	1	1	1	-1	0.91	0.74±28
8	-1	-1	-1	-1	-1	-1	-1	0.57	0.49±72
9	0	0	0	0	0	0	0	0.63	0.53±07

Table 6. Estimated regression coefficients for optimization of SNPs biosynthesis using Plackett-Burman design.

Variables	Main effect	<i>t</i> -value	<i>p</i> -value	Confidence level (%)
pH	0.522	12.787	0.000	99.978
Temp.	0.610	1.985	0.000	97.484
AgNO ₃ concentrate	0.865	14.132	0.000	99.912
Agitation	0.291	6.348	0.000	98.729
Time of incubation	0.523	7.392	0.000	97.365
Ratio	-0.740	-9.105	0.000	99.953
DV	-0.127	-0.276	0.036	86.511

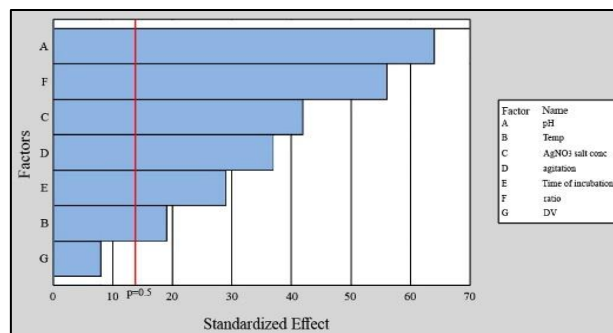


Fig. 6. The main effects of the process variables on SNPs biosynthesis by *F. oxysporum* PUN43 according to the Plackett-Burman experimental results.

Antifungal activity

The antifungal activity of the synthesized SNPs was assessed against two mycotoxigenic fungi *A. flavus* KSU 107 (peanut) and *A. parasiticus*, C009 (corn) Fig. 7. The results proved the ability of the synthesized SNPs by *F. oxysporum* PNU43 and *F. solani* PNU 54 to inhibit fungal growth with different level. The MIC which caused zero fungal growth of *A. flavus* and *A. parasiticus* was statistically resulted from the linear regression model fit. Four equations were resulted,

F. oxysporum PNU43, $Y = -1.29X + 61.44$, $R^2 = 0.81$ (*A. flavus*), $Y = -1.37X + 82.19$, $R^2 = 0.87$ (*A. parasiticus*)

F. solani PNU54, $Y = -1.17X + 43.09$, $R^2 = 0.83$ (*A. flavus*), $Y = -1.48X + 59.24$, $R^2 = 86$ (*A. parasiticus*)

In the case of *A. flavus* had MIC values of 49 and 47 mg/mL for PNU43 and PNU54. *A. parasiticus* the deduced MIC values were 49 and 48 mg/mL for PNU43 and PNU54. SNPs had an antifungal superiority on plant pathogenic fungi especially mycotoxigenic, *A. alternata*, *A. ochraceus*, *A. flavus*, *A. parasiticus* [4,16,62,63]. The SNPs antifungal activity depend on small size of particles due to easy and fast penetration of the microbial cells [64].

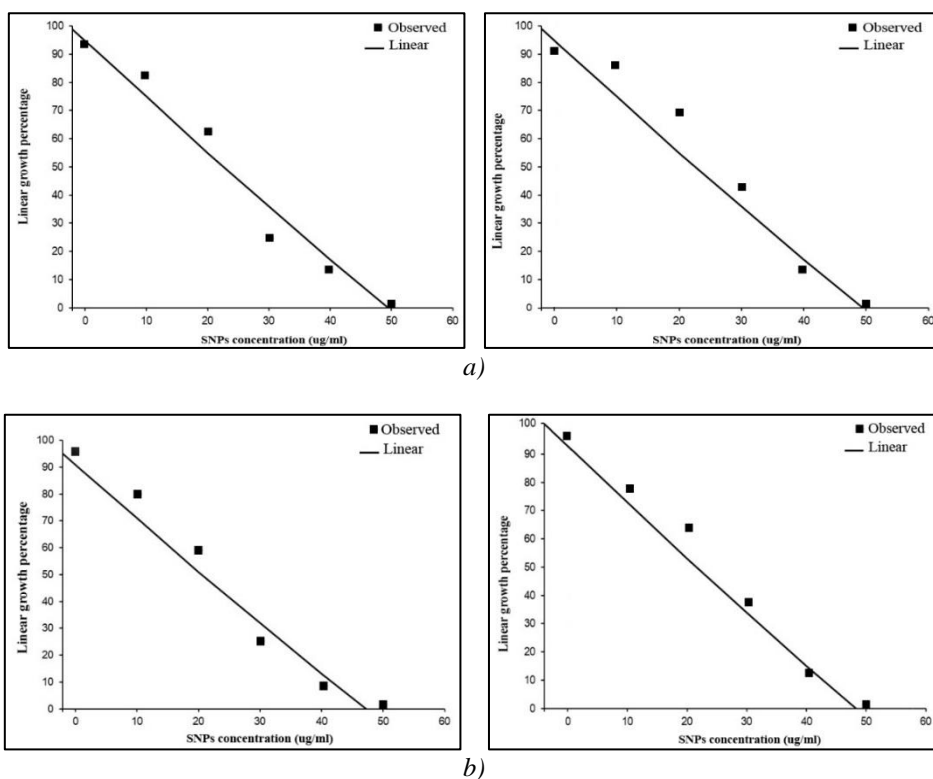


Fig. 7. Linear regression model fit of fungal growth of 1: *A. flavus* KSU 107 and 2: *A. parasiticus*, C009, as a function of, a: *F. oxysporum* PUN43 and b: *F. solani* PUN 54, producing SNPs.

Leakage of proteins and DNA:

The results in Fig. 8 show that the presence of SNPs synthesized by *F. oxysporum* PNU43 with different concentrations of in the spore suspension caused leakage of proteins as well as DNA. The results in Figure 8a at *A. flavus* case, show that high concentration 50ug/ml (OD 2.21) more effective than 10 ug/ml (OD 1.18) in the case of protein leakage. The same trend for *A. parasiticus* but *A. parasiticus* was more susceptible to the leakage of proteins. The leakage of DNA (Figure 8b) from *A. parasiticus* spore cells was higher in the case of 50ug/ml (OD 3.08) than for 10 ug/ml (OD 2.41). Generally, *A. parasiticus* was more susceptible to the leakage of proteins and DNA than *A. flavus*.

SNPs were synthesized by cell-free cultures of *F. chlamydosporum* (FAGNPs) and *P. chrysogenum* AgNPs (PAGNPs). PAGNPs were more effective than FAGNPs in causing cellular membrane damage followed the leakage of DNA and proteins against spore suspension of *A. flavus* and *A. ochraceous* [17,65]

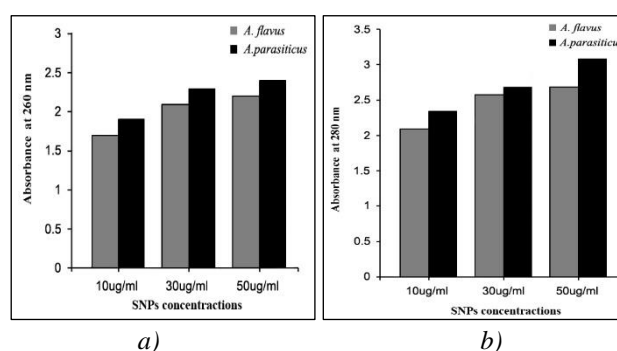


Fig. 8. Effect of SNPs synthesized by *F. oxysporum* PUN43 with different concentrations in the spore suspension caused leakage of proteins (a) and DNA (b).

Effect of SNPs on the amount of total aflatoxin

The results displayed in Fig. 9 that the statistical MIC values for complete inhibition of the total AFs production by *A. flavus* KSU 107 were 63 and 60 for PNU43 and PNU54, respectively. The MIC values inhibiting the production of total AFs production by *A. parasiticus*, C009 were 60 and 57 for PNU 43 and PNU 54, respectively. (Fig. 10) showed that HPLC chromatograms of B1 determined in liquid medium control and treated with 30 and 50 ug/ml of SNPs solution.

To our knowledge, there is no clear and accurate information in the literature concerning the effect of SNPs on aflatoxin B1 production. Three genes *pkSA*, *ver-1* and *omt-A* encode enzyme proteins were involved in the AF biosynthetic pathway. *A. flavus* ATCC 28542 treated by three different sources of SNPs, only two kinds had very good efficacy against these genes than control sample by using quantitative real-time RT-PCR of aflatoxin B1 pathway [66]. SNPs could stimulate the fungal mycelia to release O_2^- rapidly; O_2^- is playing a key role in the quick reduction of intracellular reactive oxygen species (ROS) level. The low intracellular oxidative level effect on the signaling pathway to the aflatoxin biosynthesis. Finally, the aflatoxins production by *A. flavus* is significantly suppressed [67]. The SNPs synthesized by *A. terreus* (KR364880) and *P. expansum* (KR269857) at a concentration of 220 mg/100 mL of media exhibited the highest ochratoxin A reduction, with respective percentages of 58.87 and 52.18% [4].

SNPs had highly efficient at three different concentrations on B1 production with three aflatoxigenic isolates of *A. flavus* in SMKY medium. Inhibition percentage of aflatoxin B1 production at 50ppm of SNPs ranged from 48.2 to 61.8%, at 100ppm ranged from 46.1 to 82.2% whereas at 150ppm inhibition % reached to 100% [16].

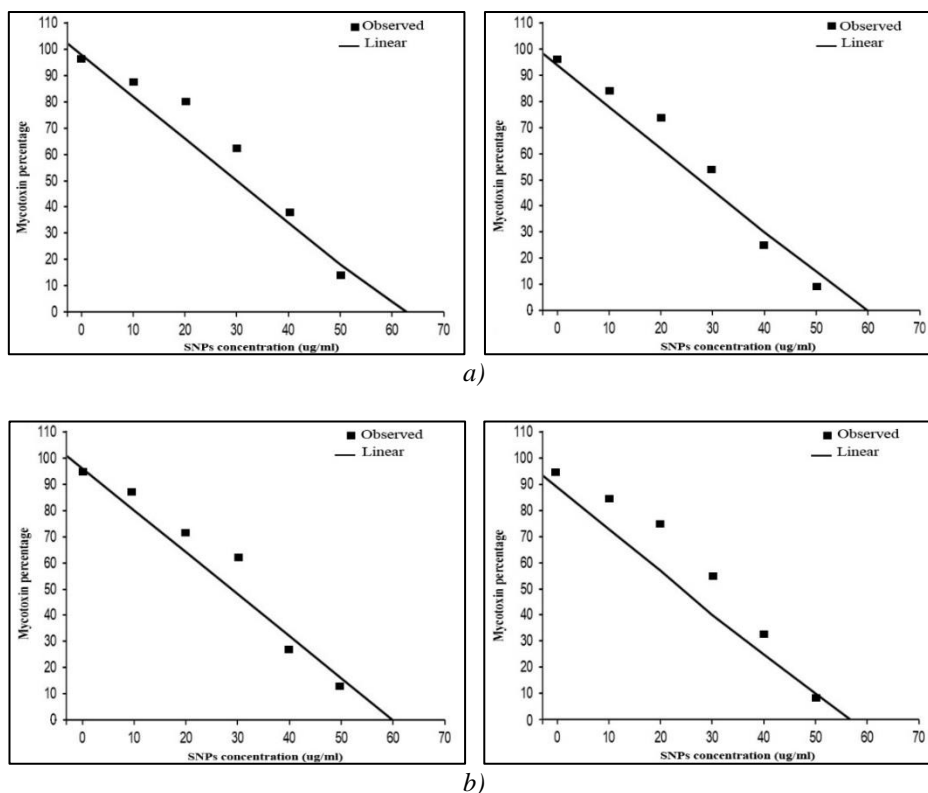


Fig. 9. Linear regression model fit of total aflatoxins production of 1: *A. flavus* KSU 107 and 2: *A. parasiticus*, C009, as a function of, a: *F. oxysporum* PUN43 and b: *F. solani* PUN 54, producing SNPs.

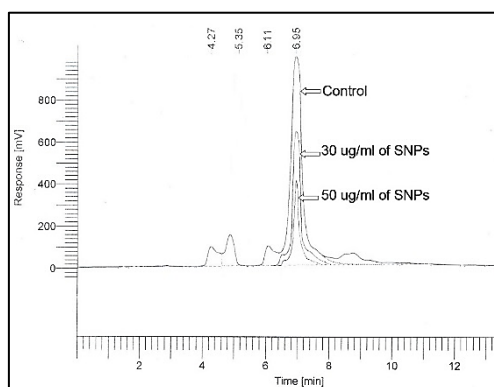


Fig. 10. HPLC chromatograms of B1 determined in liquid medium control and treated with 30 and 50 ug/ml of SNPs solution.

Fatty acid profiles

The utility of fatty acid methyl ester (FAME) profiles for characterization and differentiation of 15 isolate of *Fusarium* spp. FA profiles for each *Fusarium* isolate. are summarized in Table 7; the chain lengths of the FAs present in each *Fusarium* isolates ranged from 14 to 20 carbons. Most isolates possess a similar FA composition, with varying concentrations of FAs. The most common and abundant FAs extracted were stearic (C18:0), oleic acid (C18:1) and linoleic acid (C18:2), which comprised 90% or more of the total peak area for the three *Fusarium* species studied.

Whole cellular fatty acid compositions of 15 isolates tested were compared by conducting average linkage cluster analysis based on the ten fatty acids detected. The dendrogram produced

from the detected fatty acids showed that the clustering was unrelated to producing and non-producing SNPs (Fig. 11).

Based on the data of variations and components of fatty acids, comparison of FAME profiles among isolates of *Fusarium* spp., were carried out using principal component analysis (PCA). Comparison of the individual composition of fatty acids detected from the tissue of isolates was subjected to an analysis of variance (ANOVA).

A PCA plot of the FAME profiles generated from 15 isolates of *Fusarium* spp is shown in Figure 12. Good discrimination was obtained by the results from PCA analysis at the most clearly separated into three groups. The first group comprised 5 isolates of *F. solani*, second group included 6 isolates of *F. oxysporum*, third group contented 4 isolates of *F. verticillioides*.

Cellular FA composition is now routinely used for the identification and differentiation of micro-organisms [68]; in particular, FA profiles have recently been used as a chemotaxonomic tool for the identification and classification of bacteria [69]. Additionally, FA-based characterization is increasingly being used to distinguish between numerous species of fungi such as *Fusarium* spp. [24], *Aspergillus* spp. [70] and *Penicillium* spp. [71].

Table 7. Fatty acid profiles of the three *Fusarium* species.

<i>Fusarium</i> spp.	% of total fatty acid content (mean \pm S.D.)										
	C _{14:0}	C _{15:0}	C _{16:0}	C _{16:1}	C _{17:0}	C _{17:1}	C _{18:0}	C _{18:1}	C _{18:2}	C _{18:3}	C _{20:0}
<i>F. oxysporum</i>											
PNU41	0.95 \pm 0.51	0.42 \pm 0.05	11 \pm 0.1 6	1.13 \pm 0.43	0.37 \pm 0.12	0.67 \pm 0.26	5.21 \pm 0.72	16.39 \pm 0.71	24.75 \pm 0.34	0.19 \pm 0.06	00.00
PNU42	1.02 \pm 0.67	0.57 \pm 0.24	18 \pm 0.9 2	1.36 \pm 0.17	0.51 \pm 0.19	0.45 \pm 0.21	4.40 \pm 0.58	19.52 \pm 0.75	20.85 \pm 0.35	0.22 \pm 0.08	00.00
PNU43	1.15 \pm 0.89	0.19 \pm 0.11	13 \pm 0.8 1	0.94 \pm 0.12	0.49 \pm 0.08	0.61 \pm 0.14	7.67 \pm 0.84	17.44 \pm 0.07	18.43 \pm 0.04	0.23 \pm 0.12	00.00
PNU44	0.79 \pm 0.17	0.32 \pm 0.21	17 \pm 0.5 0	1.72 \pm 0.76	0.27 \pm 0.09	0.48 \pm 0.07	3.79 \pm 0.16	20.63 \pm 0.35	23.95 \pm 0.81	0.20 \pm 0.10	00.00
PNU45	0.93 \pm 0.45	0.46 \pm 0.14	20 \pm 0.0 9	1.54 \pm 0.19	0.21 \pm 0.13	0.33 \pm 0.17	4.87 \pm 0.73	19.17 \pm 0.92	25.59 \pm 0.05	0.11 \pm 0.03	00.00
PNU46	0.81 \pm 0.32	0.29 \pm 0.09	15 \pm 0.2 9	0.91 \pm 0.41	0.32 \pm 0.15	0.49 \pm 0.12	5.18 \pm 0.69	15.89 \pm 0.33	23.41 \pm 0.87	0.25 \pm 0.0	00.00
<i>F. solani</i>											
PNU51	0.64 \pm 0.19	0.32 \pm 0.10	24.69 \pm 0.37	1.43 \pm 0.27	00.00	0.37 \pm 0.15	5.64 \pm 0.31	21.85 \pm 0.47	29.16 \pm 0.86	0.66 \pm 0.13	2.84 \pm 0.32
PNU52	0.45 \pm 0.08	0.39 \pm 0.17	21.66 \pm 0.90	1.52 \pm 0.12	00.00	0.41 \pm 0.10	5.91 \pm 0.56	25.65 \pm 0.84	27.22 \pm 0.67	0.69 \pm 0.22	1.09 \pm 0.19
PNU53	0.55 \pm 0.14	0.26 \pm 0.09	29.75 \pm 0.28	1.57 \pm 0.06	00.00	0.69 \pm 0.29	7.16 \pm 0.88	21.15 \pm 0.63	28.53 \pm 0.37	0.73 \pm 0.09	2.17 \pm 0.29
PNU54	0.69 \pm 0.25	0.38 \pm 0.19	24.98 \pm 0.29	1.68 \pm 0.37	00.00	0.48 \pm 0.14	6.57 \pm 0.48	24.91 \pm 0.21	29.23 \pm 0.42	0.51 \pm 0.19	2.73 \pm 0.12
PNU55	0.47 \pm 0.18	0.29 \pm 0.11	20.36 \pm 0.62	1.69 \pm 0.15	00.00	0.51 \pm 0.07	4.91 \pm 0.07	25.79 \pm 0.14	21.87 \pm 0.31	0.48 \pm 0.17	1.79 \pm 0.23
<i>F. verticillioides</i>											
PNU61	0.56 \pm 0.11	0.75 \pm 0.12	14 \pm 0.5 9	1.82 \pm 0.16	00.00	1.16 \pm 0.21	5.8 \pm 0 .73	19.36 \pm 0.24	23.54 \pm 0.73	1.79 \pm 0.14	00.00
PNU62	0.61 \pm 0.13	0.78 \pm 0.23	12 \pm 0.4 8	1.91 \pm 0.55	00.00	1.06 \pm 0.18	5.1 \pm 0 .44	19.71 \pm 0.19	25.65 \pm 0.83	1.52 \pm 0.27	00.00
PNU63	0.53 \pm 0.09	0.69 \pm 0.19	15 \pm 0.3 1	1.74 \pm 0.47	00.00	1.39 \pm 0.15	5.4 \pm 0 .59	21.29 \pm 0.77	24.91 \pm 0.36	1.16 \pm 0.13	00.00
PNU64	0.51 \pm 0.10	0.66 \pm 0.24	17 \pm 0.6 2	1.86 \pm 0.36	00.00	1.24 \pm 0.23	5.3 \pm 0 .28	21.83 \pm 0.38	24.44 \pm 0.25	1.43 \pm 0.16	00.00

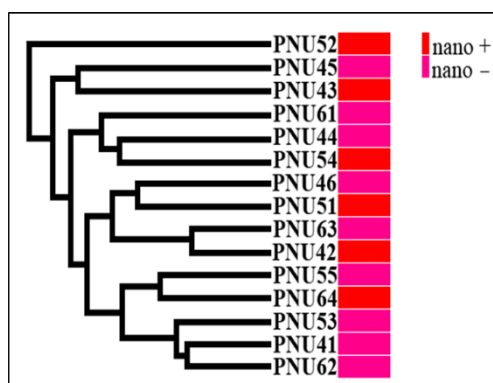


Fig. 11. Dendrogram showing relationships among 15 isolates of *F. oxysporum*, *F. solani* and *F. verticillioides* based on the analysis of fatty acid methyl ester (FAME) profiles.

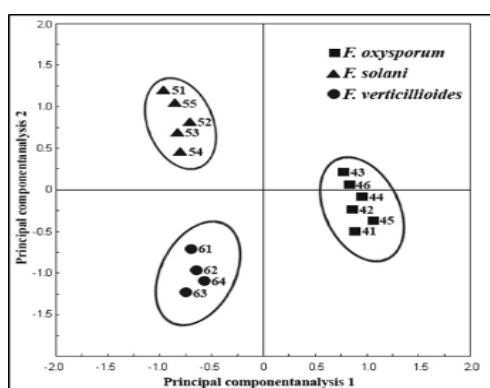


Fig. 12. Relationship of fatty acid methyl ester (FAME) profiles among 15 isolates of *Fusarium* spp., as represented by plots of the first two principal component analyses.

ISSR analysis

Out of the 50 primers used, 24 primers that produced unambiguous fragments with repeatable patterns when tested with three *Fusarium* spp (Table 2). Over the 8 primers, the fragment size obtained from *F. oxysporum* isolates ranged from 200 bp to 2200 bp and a total of 61 amplified bands (loci) were generated, with an average of 8 bands per primer. In case of *F. solani* showed total of 88 amplified bands, with an average of 11 bands per primer. Eight primers generated an average of 9 bands amplified by each primer and total bands was 68 when using *F. verticillioides* isolates.

Most markers produced polymorphisms; percentage polymorphism was calculated by considering the amount of polymorphism produced per fragment. $(AG)_8T$, $(GA)_8C$ and $(AC)_8T$ (*F. oxysporum*), $(AG)_8T$ and $(AG)_8YC$ (*F. solani*), $(GA)_8T$, $(CT)_8AC$, $(ATG)_6$ and $(CCA)_6$ (*F. verticillioides*) showed 100% polymorphism, where $(AC)_8T$ generated maximum number of fragment (Fig. 13).

The ISSR data to assess the genetic relatedness among the *Fusarium* spp. (Fig. 14). The ISSR data of six isolates *F. oxysporum* showed a similarity coefficient (SC) ranging from 0.60 to 0.92 by using primer UBC 809 $(AG)_8G$ (Fig. 14a). Cluster I accommodated PNU42 and PNU43 (both producing SNPs) while cluster II comprised PNU46, PNU44, PNU41 and PNU45 (non-producing SNPs).

UPGMA dendrogram based on the similarity matrix for five isolates of *F. solani* with UBC 809 displayed the SCs ranged from 0.72% to 0.91 between the isolates (Fig. 14b). Cluster I had PNU52 and PNU54 (both producing SNPs), while cluster II comprised PNU55, PNU53, (non-producing SNPs) and PNU51 (producing SNPs).

A cluster analysis of four isolates *F. verticillioides* was performed based on the similarity matrix with primer UBC 809, which showed that the SC ranged from 0.87% to 0.94 (Fig. 14c). Cluster I had PNU61 and PNU62 (non-producing SNPs) and (producing SNPs), while cluster II comprised PNU64 (producing SNPs), PNU63 (non-producing SNPs).

ISSR markers were used with the aim of genetically characterizing 15 isolates of *Fusarium* spp. and discriminate between producing and non-producing SNPs isolates. In general, there was no clear-cut relationship between the genotype of isolates, antifungal and anti-aflatoxin properties.

Only two papers focused on this point, two papers using ISSR markers with *Aspergillus* spp. ISSR molecular marker made possible the detection of inter- and intraspecific genetic variation, which is actually very useful as an auxiliary tool for genetic characterization of *Aspergillus* spp producing and non-producing SNPs [72,73].

ISSR molecular technique generated highly polymorphic markers that could be used to study *F. verticillioides* genetic characterization of *F. oxysporum* [42], *F. solani* [43] and *F. verticillioides* [44] to clarify phylogenetic relationships.

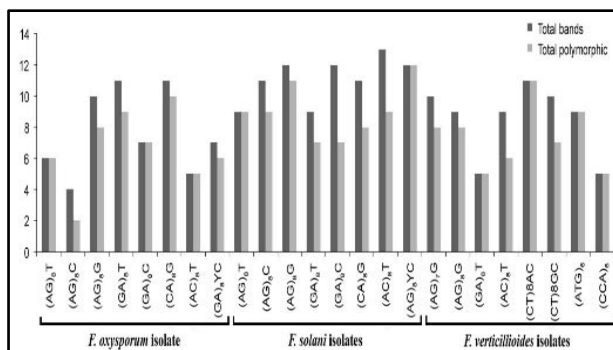


Fig. 13. Bar graph showing various fragments produced by primers and total polymorphisms produced by them.

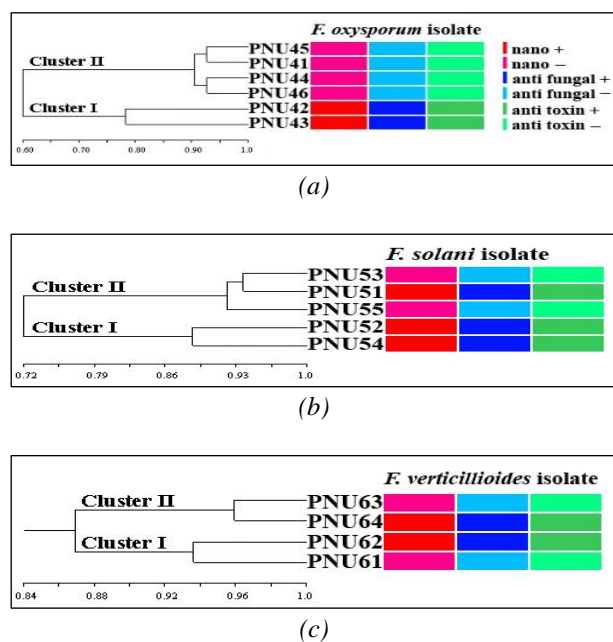


Fig. 14. UPGMA dendrogram based on Jaccard's coefficient illustrating the genetic similarities among *Fusarium* spp. based on ISSR data. a) six isolates of *F. oxysporum*, b) five isolates of *F. solani*, c) four isolates of *F. verticillioides* with primer UBC811.

Conclusions

It can be concluded that *Fusarium* spp. is an excellent fungal resource for the biosynthesis of SNPs. The biosynthesized SNPs were characterized by UV–Vis spectrophotometry, Fourier transform infrared spectroscopy (FTIR), X-ray diffraction (XRD), transmission electron microscopy (TEM). Statistical optimization of fermentation conditions using Plackett-Burman design and Box-Behnken design appears to be a valuable tool for the production of SNPs by *Fusarium* spp.

The antifungal activity of SNPs was studied against mycotoxigenic fungi such as *A. flavus* and *A. parasiticus*, also effectiveness in reducing AFs production by *A. flavus* and *A. parasiticus*. ISSR-PCR is a perfect tool for molecular characterization and high genetic diversity among the *Fusarium* spp. isolates. Cluster analysis of ISSR markers revealed no clear grouping of the isolates producing and non-producing SNPs.

Acknowledgement

This research project was funded by the Deanship of Scientific Research, Princess Nourah Bint Abdulrahman University, through the Research Group Funding Program, grant No. 29 – ص – 235.

References

- [1] Li. Xiangqian, Xu. Huizhong, Chen. Zhe-Sheng, Chen. Guofang, Journal of Nanomaterials, Article ID 270974, 1 (2011).
- [2] S. Gaikwad, S. Birla, A. Ingle, A. Gade, Journal of the Brazilian Chemical Society **24**, 1974 (2013).
- [3] A. R. M. Abd El-Aziz, M. R. Al-Othman, S. A. Eifan, M. A. Mahmoud, Digest Journal of Nanomaterials and Biostructures **8**, 1215 (2013).
- [4] H. A. Ammar, T. A. El-Desouky, Journal of Applied Microbiology **121**, 89 (2016).
- [5] R. M. Elamawi, R. E. Al-Harbi, A. A. Hendi, Egyptian Journal of Biological Pest Control **28**, 28 (2018).
- [6] S. I. Abdel-Hafez, N. A Nafady, I. R. Abdel-Rahim, A. M. Shaltout, 3 Biotech. **6**, 199 (2016)
- [7] S. S. Birla, S. C. Gaikwad, A. K. Gade, M. K. Rai, The Scientific World Journal **2013**, 1 (2013)
- [8] P. I. Nikel, M. J. Pettinari, B. S. Mendez, M. A. Galvagno, International Microbiology **8**, 243 (2005)
- [9] R. L. Plackett, J. P. Burman, Biometrika **33**, 305 (1946).
- [10] P. Balaure C. Gudovan, D. Gudovan, New Pesticides and Soil Sensors **2017**, 129 (2017).
- [11] J. Hayles, L. Johnson, C. Worthley, D. Losic, New Pesticides and Soil Sensors **2017**, 193 (2017).
- [12] C. G. Athanassiou, N. G. Kavallieratos, G. Benelli, D. Losic, P. U. Rani, N. Desneux, Journal of Pest Science **91**, 1, (2018).
- [13] G. Benelli, Parasitology Research **115**, 23 (2016)
- [14] G. Gonzalez, M. J. Hinojo, R. Mateo, A. Medina, International Journal of Food Microbiology **15**, 1 (2005).
- [15] F. N. Kotsonis, G. A. Burdock, W. G. Flamm, Food toxicology. In: Casarett and Doull's Toxicology: The Basic Science of Poisons. Klases CD (ed.). New York: McGraw-Hill, p. 1049, 2001.
- [16] M. R. Al-Othman, A. R. Abd El-Aziz, M. A. Mahmoud, S. A. Eifan, Digest Journal of Nanomaterials and Biostructures **9**,151 (2014).
- [17] N. Khalil, M. Abd El-Ghany, S. Rodríguez-Couto, Chemosphere **218**, 477 (2019).
- [18] G. Fourie, E. T. Steenkamp, T. R. Gordon, A. Viljoen, Applied and Environmental Microbiology **75**, 4770 (2009).
- [19] I. Schmitt, A. Crespo, P. Divakar, J. Fankhauser, Persoonia **23**, 35 (2009).
- [20] M. Kvas, W. Marasas, B. Wingfield, M. Wingfield, Fungal Diversity **1**, 1 (2009).
- [21] M. Diamond, T. Reape, O. Rocha, S. Doyle, Plos one **8**, e69542 (2013).
- [22] Samson, R., C. M. Visagie, J. Houbraken, Studies in Mycology **78**, 141 (2014).
- [23] J. C. Frisvad, T. O. Larsen, R. de Vries, Studies in Mycology **59**, 31 (2007).
- [24] M. E. Zain, A. H. Bahkali, M. R. Al-Othman, African journal of microbiology **7**, 4638 (2013).
- [25] Y. Shao, L. Xu, F. Chen, Mycoscience **52**, 224 (2011).
- [26] X. Huang, X. Zhang, L. Huang, Biochemical Systematics and Ecology **57**, 338 (2014).

- [27] Baysal, Ö. M. Siragusa, E. Gümrükcü, S. Zengin, *Biochemical Genetics* **48**,524 (2010).
- [28] M. A. Mahmoud, A. R. M. Abd El-Aziz, *Research journal of biotechnology* **11**, 53 (2016).
- [29] S. A. Waksman, E. B. Fred, *Soil Science* **14**, 27 (1922).
- [30] K. H. Domsch, W. Gams, T. H. Anderson, *Compendium of Soil Fungi*, vol. I. pp. 859. Berlin: IHW-Verlag, (1993).
- [31] P. E. Nelson, T. A. Toussoun, W. F. Marasas, *Fusarium species: an illustrated manual for identification*, The Pennsylvania St. Univ, p. 193, (1983).
- [32] O. E. Amer, M. A. Mahmoud, A. M. El-Samawaty, S. R. Sayed, *African journal of biotechnology* **10**, 14337 (2011).
- [33] T. J. White, T. Bruns, S. Lee, J. Taylor, Amplification and direct sequencing of fungal ribosomal RNA genes for phylogenetics. In: Innis M., Gelfand D., Sninsky J., White T. (eds): *PCR Protocols: a Guide to Methods and Applications*. Orlando, Academic Press: 315 (1990).
- [34] K. Tamura, G. Stecher, D. Peterson, A. Filipiński, S. Kuma, *Molecular Biology and Evolution* **30**, 2725 (2013).
- [35] M. A. Mahmoud, S. A. Al-Sohaiban, M. R. Al-Othman, A. R. M. Abd El-Aziz, *Digest Journal of Nanomaterials and Biostructures* **8**, 589 (2013).
- [36] Y. S. Chan, M. M. Don, *Materials Science and Engineering C* **33**, 282 (2013).
- [37] G. Singhal, R. Bhavesh, K. Kasariya, A. R. Sharma, *Journal of Nanoparticle Research* **13**, 2981 (2011).
- [38] N. El-Naggar, A. Mohamedin, S. Hamza, A. Sherief, *Journal of Nanomaterials* **2016**, 1 Article ID 3257359, (2016)
- [39] E. B. El Domany, T. M. Essam, A. E. Ahmed, A. A. Farghali, *Journal of Applied Pharmaceutical Science* **8**, 119 (2018).
- [40] C. Gertz, 1990. *HPLC Tips and Tricks*. Great Britain at the Iden Press, Oxford.
- [41] G. Lepage, C. C. Roy, *The Journal of Lipid Research* **27**, 114 (1986).
- [42] M. Katkar, S. Mane, N. Kadam, *Legume Research* **38**, 246 (2015).
- [43] S. Shahnazi, S. Meon, G. Vadamalai, D. Yazdani, *Pertanika Journal of Tropical Agricultural Science* **37**, 359 (2014).
- [44] Divakara, S., P. Santosh, M. Aiyaz, M. Ramana, *Journal of the Science of Food and Agriculture* **94**, 1132 (2013).
- [45] M. Bogale, B. D. Wingfield, M. J. Wingfield, E. T. Steenkamp, *Fungal Diversity* **23**, 51 (2006).
- [46] L. W. Burgess, *General ecology of the Fusaria*. In: Nelson, P. E., Toussoun, T. A., Cook, R.J. (Eds.), *Fusarium: Disease, Biology, and Taxonomy*. The Pennsylvania University Press, University Park, p. 225 (1981).
- [47] I. Ahmed, M. Abid, F. Hussain, S. Abbas, *International Journal of Biology and Biotechnology* **13**, 33 (2016).
- [48] S. F. Manzelat, *International Journal of Soil Science* **20**, 1 (2017).
- [49] X. Zeng, F. Kong, C. Halliday, S. Chen, *Journal of Clinical Microbiology* **45**, 2872 (2007).
- [50] M. Dita, C. Waalwijk, I. Buddenhagen, M. Souza, 2010. *Plant Pathology* **59**, 348 (2010).
- [51] P. Azmath, S. Baker, D. Rakshith, S. Satish, *Saudi Pharmaceutical Journal* **24**, 140 (2016).
- [52] S. Anbazhagan, S. Azeez, G. Morukattu, R. Rajan, *3Biotech* **7**, 333 (2017).
- [53] A. Ahmad, S. Senapati, M. Khan, K. Rajiv, 2003. *Nanotechnology* **14**, 824 (2003).
- [54] P. Mukherjee, M. Roy, B. Mandal, G. Dey, *Nanotechnology* **19**, 103 (2008).
- [55] N. Jain, C. Bhargava, A. Majumdar, J. Tarafdar, *Nanoscale* **3**, 635 (2011).
- [56] Y. Zhao Y. Jiang, Y. Fang, *Acta Part A: Molecular and Biomolecular Spectroscopy* **65**, 1003 (2006).
- [57] S. Solomon, M. Bahadory, A. Jeyarajasingam, S. Rutkowsky, *Journal of Chemical Education* **84**, 322 (2007).
- [58] A. Nair, T. Pradeep, *Current Science* **84**, 1560 (2003).
- [59] A. Gole, C. Dash, V. Ramakrishnan, S. Sainkar, *Langmuir* **17**, 1674 (2001).
- [60] D. Balaji, S. Basavaraja, R. Deshpande, D. Bedre, *Colloids and Surfaces B: Biointerfaces* **68**, 88 (2009).
- [61] G. Li, D. He, Y. Qian, B. Guan, *International Journal of Molecular Sciences* **13**, 446 (2012).
- [62] A. M. Abdel-Hadi M. F. Awad, N. F. Abo-Dahab, M. F. ElKady, *Biosciences, Biotechnology Research Asia* **11**, 1179 (2014).
- [63] S. A. Mousavi, S. Pourtalebi, *The Iranian Journal of Medical Sciences* **40**, 501 (2015).
- [64] F. Martinez-Gutierrez, P. Olive, A. Banuelos, E. Orrantia, *Nanomedicine* **6**, 681 (2010).
- [65] S. M Dizaj, F. Lotfipour, M. Barzegar-Jalali, M. H. Zarrintan, *Materials Science and Engineering: C* **44**, 278 (2014).
- [66] M. M. Deabes, W. K. Khalil, A. G. Attallah, T. A. El-Desouky, *Open Access Macedonian Journal of Medical Sciences* **6**, 600 (2018).
- [67] J. Zhao, L. Wang, D. Xu, L. Zhisong, *RSC Advances* **7**, 23021 (2017).

- [68] P. Devi, M. Shridhar, L. Souza, *Indian Journal of Marine Sciences* **35**, 259 (2006).
- [69] R. B. Cody, C. R. McAlpin, C. R. Cox, *Rapid Communications in Mass Spectrometry* **29**, 2007 (2007).
- [70] M. E. Fraga, D. M. Santana, M. J. Gatti, *The Memórias do Instituto Oswaldo Cruz* **103**, 540 (2008).
- [71] M. A. Mahmoud, A. R. M. Abd El-Aziz, M. R. Al-Othman, *Biotechnology & Biotechnological Equipment* **30**, 1090 (2016).
- [72] M. A. Mahmoud, A. R. M. Abd-El-Aziz, M.R. Al-Othman, *Research journal of biotechnology* **10**, 73 (2015).
- [73] A. R. M Abd El-Aziz, M. R. Al-Othman, M.A. Mahmoud, S. A. Moner, *Digest Journal of Nanomaterials and Biostructures* **10**, 31 (2015).